

21 **ABSTRACT**

22 In the dry-cured ham industry, an accurate control of the dry-salting process is  
23 especially complex because of the great heterogeneity of the meat pieces and the  
24 effect of different operational variables. The main objective of this study was to  
25 evaluate the feasibility of using an ultrasound system and methodology, adapted to the  
26 industry requirements, for the online monitoring of the ham dry-salting process. For that  
27 purpose, hams were dry salted for different times (4, 10, 11, 14, 16 and 30 days) at  
28 2°C. The cushion zone of the ham was placed over the transducers during salting and  
29 ultrasonic signals were taken automatically (5 min interval by using pulse-echo mode.  
30 Several methods of signal analysis were considered in order to assess the time of flight  
31 (TOF). TOF estimations by means of the energy threshold and cross-correlation  
32 methods (between the initial ultrasonic signal and the remaining signals measured  
33 during salting and between consecutive signals 5 min apart without interpolation) were  
34 affected by the low signal-to-noise ratio and the pulse distortion and were discarded for  
35 the online monitoring of ham salting. Otherwise, the cross-correlation method between  
36 consecutive signals (5 min apart) with interpolation  $n=3$  (CCM-CS  $n=3$ ), between non-  
37 consecutive signals (1 h apart) (CCM-NCS) and the phase spectrum method (PSM),  
38 provided close estimations of the variation of the TOF, which correlated well with the  
39 ham salt gain ( $R^2=0.83$  for CCM-CS  $n=3$ , 0.93 for CCM-NCS and 0.90 for PSM).  
40 Consequently, the use of ultrasonic pulse-echo TOF measurements could be  
41 considered as a simple, non-invasive, non-destructive and reliable technique for the  
42 industrial monitoring of the ham dry-salting process.

43 **Keywords:** *Salting; Ham; Time of flight; Energy threshold; Cross-correlation; Phase*  
44 *spectrum*

45

## 46 **1. INTRODUCTION**

47 The online monitoring of food processes allows the physicochemical changes that take  
48 place in food matrices during manufacturing to be controlled, in order to achieve the  
49 expected organoleptic and safety attributes. Nowadays, several new non-destructive  
50 techniques (X-Rays, NIR spectroscopy, ultrasound, etc.) have been developed or  
51 adapted for the purposes of measuring a wide range of quality parameters during food  
52 processing (Dixit et al., 2017; Perez-Santaescolastica et al., 2019).

53 In dry-cured ham manufacturing, the dry-salting stage consists of stacking the hams,  
54 subcutaneous fat side down, surrounded by coarse salt at 2-4°C and a relative  
55 humidity of 90-95% for several days (Toldra, 2010). At present, the salting time is  
56 mainly determined from the average weight of the hams, which have previously been  
57 separated into batches of similar weight. The monitoring of the dry-salting process  
58 would be of great interest for the meat industry, since the salt gain in a batch of hams  
59 varies widely, because of the great heterogeneity of the meat pieces (composition,  
60 shape and structure) and the effect of the different operational variables (De Prados et  
61 al., 2015). This variable salt gain causes non-uniform behaviour of the hams during the  
62 subsequent processing stages, and consequently, the final dry-cured hams from the  
63 same batch have heterogeneous sensory properties, affecting their quality.

64 Low-intensity ultrasound is one of the most promising non-invasive technologies for  
65 food process monitoring since it is accurate, fast, easy to implement on-line and  
66 relatively inexpensive. In this regard, the ultrasonic measurements have been used to  
67 monitor a wide range of food processes, such as the rennet of whole milk during  
68 cheese manufacturing (Koc and Ozer, 2008), the alcoholic fermentation in synthetic  
69 broths (glucose, fructose and sucrose) and in natural media (must and wort) (Resa et  
70 al., 2009), the temperature and the ice content of fish (hake) during freezing (Aparicio  
71 et al., 2008), the ripening of tofu (Ting et al. 2009), the quality of oil during frying  
72 (Benedito et al., 2002) or the crystallization of palm oil in O/W emulsions (Awad and

73 Sato, 2002). Recently, De Prados et al. (2016) used the ultrasonic through-  
74 transmission technique to monitor the pork meat dry-salting process (*Biceps femoris*  
75 and *Longissimus dorsi* muscles). In most of these studies, ultrasonic velocity,  
76 calculated from the time of flight (TOF) and the sample thickness, is the parameter  
77 calculated from the ultrasonic signal and chosen for the purposes of correlation with  
78 compositional and mechanical properties. The accurate estimation of other ultrasonic  
79 parameters, such as attenuation, results very complicated in solid foods if coupling  
80 materials, such as gels, are not used. The use of coupling materials has some  
81 disadvantages, which strongly prevents their application in many cases because it may  
82 involve the product's surface contamination, as well as the slowdown of the  
83 measurement.

84 Overall, the energy threshold method is the one most often used to determine the TOF  
85 from the ultrasonic signals. However, when the signal in the sample has a low signal-  
86 to-noise ratio (SNR) and/or a large pulse distortion, this method can lead to a  
87 miscalculation of the TOF, and other approaches, such as the cross-correlation and  
88 phase spectrum methods, must be considered (Sachse and Pao, 1978; Leemans and  
89 Destain, 2009; Pallav and Hutchins, 2009). Alternatively, when the different echoes  
90 overlap in the time domain, amplitude spectrum methods can be used (Pialucha et al.,  
91 1989; Gomez Alvarez-Arenas, 2009a and 2009b; Sarabia et al., 2013). Moreover,  
92 when the material under study is dispersive, cross-correlation methods can only be  
93 applied to sufficiently large tone bursts.

94 De Prados et al. (2016) used the through-transmission method for the online  
95 monitoring of the dry-salting of meat muscles, placing two transducers on the opposite  
96 sides of the product. This set-up allows good signal amplitude to be obtained, since the  
97 ultrasonic wave has to cross the sample only once. However, this configuration could  
98 lead to important drawbacks when implemented for the online monitoring of the dry-  
99 salting of hams, since transducers have to be located on both faces of the stacked  
100 hams and perfectly aligned during the whole salting process. An alternative

101 configuration might be the use of transducers located at the bottom of the stack of  
102 hams and working in the pulse-echo mode. However, using this simple and easy-to-  
103 implement online arrangement, the ultrasonic signal has to cross a thick, highly  
104 heterogeneous and complex medium composed of skin, bones and different muscles  
105 twice, which could hinder the measurement of the TOF due to a more intense  
106 attenuation and signal distortion. Therefore, the aim of this study was to investigate the  
107 feasibility of using an ultrasound pulse-echo technique, adapted to the industry  
108 requirements, for the online monitoring of the dry-salting process of hams and to  
109 determine the most adequate method for signal analysis in order to calculate the  
110 changes in the TOF during salting.

## 111 **2. MATERIALS AND METHODS**

### 112 **2.1 SAMPLES AND DRY-SALTING PROCESS**

113 *Large White* breed hams were purchased in a local market with an average weight of  
114  $13.3\pm 4.5$  kg and pH  $5.7\pm 0.1$  (FG2-FiveGo™, Mettler Toledo, US). The average fat  
115 ( $14.8\pm 4.1$  kg/100 kg) and moisture contents ( $70.5$  kg/100 kg) were measured according  
116 to AOAC (1997) standard procedures 991.36 and 950.46, respectively. Analytical  
117 determinations were carried out in the cushion zone of the ham where ultrasonic  
118 experiments were performed. In raw hams, the thickness of the cushion zone was  
119  $11.5\pm 0.4$  cm and maximum width of raw hams reached  $31.6\pm 1.3$  cm. The analysis of  
120 salting process focused on the cushion zone of the ham, which is the most critical one  
121 in terms of salting since it is the thickest part.

122 All the hams were dry-salted by covering the piece with 15kg of coarse salt (NaCl  
123 moisturized at 10% w/w) at  $2\pm 1^\circ\text{C}$  in a cold chamber (AEC330r, Infrico, Spain) in which  
124 relative humidity ranged between 80-85%. Raw hams and coarse salt were previously

125 stored for 24h at 2°C for the purpose of tempering. One ham was used for each salting  
126 time considered (4, 10, 11, 14, 16 and 30 days).

127

## 128 **2.2 ULTRASOUND EXPERIMENTAL SET-UP**

129 The ultrasonic experimental set-up was designed to develop a reliable, simple and  
130 robust methodology aiming to be further applied at industrial level. Ultrasonic  
131 measurements were during the dry-salting experiments carried out on hams. The  
132 ultrasonic experimental set-up used (Figure 1) consisted of two narrow-band  
133 piezoelectric transducers of 1MHz and 0.5" crystal diameter (T1 and T2, A303S model,  
134 Panametrics, Waltham, MA, USA), a pulser-receiver instrument (5077PR, Panametrics,  
135 Waltham, MA, USA), a digital input/output USB device (NI 6501, National Instruments,  
136 Austin, TX, USA) and a high-speed digitizer (PXI/PCI-5112, National Instruments,  
137 Austin, TX, USA) installed in a PC. Signal digitalization was started by the output  
138 trigger signal of the pulser-receiver instrument using an independent channel of the  
139 digitizer. The digital input/output device was used as a multiplexer of the excitation  
140 pulse and the received signal, so a single pulser/receiver unit was used.

141 For the purposes of taking the ultrasonic measurements, the two transducers (T1 and  
142 T2, Figure 1) were firstly embedded in a layer of 5kg of salt placed in the bottom of a  
143 plastic container (120x35x20cm). Secondly, the cushion part of the ham was placed on  
144 the layer in direct contact with the transducers' surface and the salt. Coupling materials  
145 were not used to improve the contact between the transducer and sample surface.  
146 Next, two temperature sensors (type-K thermocouples) were placed both in the salt  
147 and on the surface of the sample; and the remaining 10 kg of salt were added until the  
148 sample was entirely covered (Figure 1). The ultrasonic measurements were taken by  
149 pulse-echo mode at intervals of 5min in the cushion zone of the ham. The signal

150 received from each transducer was digitized (25kpoints at 100Msamples/s, 10% pre-  
151 trigger points) and stored for further signal analysis.

## 152 **2.3 METHODS FOR SIGNAL ANALYSIS**

153 Different signal analysis methods (energy threshold, cross-correlation and phase  
154 spectrum) were applied in order to determine which was the most appropriate as a  
155 means of calculating the time of flight (TOF) (Povey and Mason, 1998) and so  
156 monitoring the ham salting.

157 In the energy threshold method (ETM), the dead zone (zone A, Figure 2) was  
158 discarded, this can be defined as the portion of signal corresponding with the  
159 transducer's own vibration and also reflections of the ultrasonic wave on interfaces  
160 close to the transducer-ham surface interface. Thus, the TOF was calculated when the  
161 wavefront arrived at the transducer (zone B, Figure 2), when the amplitude of the  
162 received signal exceeded the established threshold (0.1V) (Sarabia et al., 2013), which  
163 was sufficiently above the existing background noise level. This method assumes no  
164 signal distortion and a good sound-to-noise ratio (SNR) and has been applied to  
165 compute ultrasonic velocity in different meat products (Nowak and Markowsky et al.,  
166 2015 and 2016). Novak and Markowsky (2013) reported that similar results are  
167 obtained by identifying the maximum amplitude of the ultrasonic signal instead of the  
168 wavefront arrival.

169 Additionally, the cross-correlation method (CCM) (Leemans and Dastain, 2009) was  
170 considered. This method calculates the time of flight variation between two similar  
171 signals ( $\Delta\text{TOF}_{2s}$ ) as follows.

172 Given two waveforms  $f(t)$  and  $g(t)$ , the cross-correlation  $(f * g)(t)$  is defined as:

$$173 \quad (f * g)(t) = \int_{-\infty}^{\infty} f^*(s) g(t + s) ds \quad (1)$$

174 where  $f^*(s)$  denotes the complex conjugate of  $f(s)$ . The discrete form of the cross-  
175 correlation function, which is the one used in this paper is:

$$176 \quad (f * g)(t) = \frac{1}{N} \sum_{n=0}^{N-1-k} f_n g_{n+k} \quad (2)$$

177 where  $f_n, g_n$  are the two N-length discrete waveforms

178 The maximum value of  $(f * g)(t)$  determines when the two signals are overlapped and the  
179 position of the maximum in the array permitted the calculation of the  $\Delta\text{TOF}_{2s}$ . In order  
180 to identify the maximum, the adoption of appropriate interpolation methods may  
181 improve the accuracy of the estimation (Svilainis, 2016).

182 Several approaches were considered to calculate the change in the time of flight from  
183 the beginning to the end of the salting experiment ( $\Delta\text{TOF}$ ). Firstly, the  $\Delta\text{TOF}_{2s}$  was  
184 calculated using the CCM between the initial or reference signal (0h salting, RS) and  
185 the signal at the salting time considered (CCM-RS). Secondly, the CCM was performed  
186 for each pair of consecutive signals (5min apart) and then the  $\Delta\text{TOF}$  for each salting  
187 time was calculated by the addition of the  $\Delta\text{TOF}_{2s}$  between consecutive signals from  
188 the beginning of salting until the salting time considered. In this case, two approaches  
189 were followed: CCM was performed on the raw signals (no interpolation; CCM-CS n=0)  
190 and on interpolated signals (3 samples' interpolation; CCM-CS n=3). Finally, the same  
191 procedure was followed, but performing the CCM between the signals that are 1h apart  
192 (CCM-NCS). CCM algorithms were programmed in Labview™ 2018 (National  
193 Instruments, Austin, TX, USA) using the available functions for cross correlation and  
194 interpolation and the signals were standardized to the maximum amplitude. The  
195 correction of DC components in the signal was not necessary.

196 Finally, a phase spectrum method (PSM), which is an adaptation of the method  
197 proposed by Sachse and Pao (1978), was used to calculate the  $\Delta\text{TOF}_{2s}$  between  
198 consecutive signals each one 5min apart. For that purpose, a square time window of  
199 fixed location and length (from 13k to 20k points) was used in every case to select the

200 portion of the B-Scan where the echo coming from the ham back surface appears. The  
 201 FFT of the signal is a complex number, whose module and phase give rise to the  
 202 module spectrum and phase spectrum, respectively. The square of the module  
 203 spectrum provides the energy of the signal at each frequency and the phase spectrum  
 204 ( $\phi$ ) is given by (Koksel et al., 2014 and 2017):

$$205 \quad \phi = \omega(t - t_0) \quad (3)$$

206 where  $\omega$  is a vector containing the discretized angular frequency values within the  
 207 signal frequency band,  $t$  the time and  $t_0$  the time origin which is, normally, set at the  
 208 centre of the time window. From the module spectrum of the signal received at the  
 209 beginning of the salting process, the system frequency band (including the frequency  
 210 band of pulser, transducers, receiver, analog-to-digital converter and the contribution of  
 211 the attenuation over the travelled distance), which is defined as the frequency band  
 212 where the module spectrum is above the threshold given by a peak value of - 6dB  
 213 (frequency window 0.85-1.04 MHz), was obtained. Given any two signals, the time  
 214 delay can be calculated from the difference between the phase spectrum of both, within  
 215 the system frequency band:

$$216 \quad \phi_1(\omega) = \omega(t_1 - t_0), \quad \phi_2(\omega) = \omega(t_2 - t_0) \quad (4)$$

$$217 \quad \Delta\phi(\omega) = \phi_1(\omega) - \phi_2(\omega) = \omega(t_1 - t_2) = \Delta t(\omega) = \Delta TOF(\omega) \quad (5)$$

218 Therefore, in this case, a time delay is obtained for every frequency value within the  
 219 system frequency band, which is why this is the only method able to cope with TOF  
 220 estimations of wideband signals in the presence of dispersion. In order to obtain a  
 221 single  $\Delta TOF_{2s}$  estimation, instead of  $\Delta TOF(\omega)$ , which can be compared with the results  
 222 obtained by the other procedures, the average value of  $\Delta TOF(\omega)$  was assessed:

$$223 \quad \Delta TOF_{2s} = \frac{\sum_{i=1}^{i=N} (\Delta TOF(\omega_i))}{N} \quad (6)$$



224 Where  $\omega_i$   $i=1,N$  is the angular frequency within the system 6-dB frequency band.

225 Finally, the  $\Delta\text{TOF}$  for each salting time was calculated by the addition of the  $\Delta\text{TOF}_{2s}$   
226 between consecutive signals from the beginning of salting until the salting time  
227 considered.

228 As well as for CCM, specific software programmed in LABVIEW™ 2015 (National  
229 Instruments, Austin, TX, USA) was used in PSM.

## 230 **2.4 CHEMICAL ANALYSIS**

231 The salt and water content were determined in the salted ham. For that purpose, two  
232 cylindrical salted samples ( $204\pm 21\text{g}$ ), which included the ultrasonic measurement  
233 zones, were taken by using a cylindrical cutter (5cm in diameter). Each cylindrical  
234 salted sample was ground and homogenized before analytical determinations. The  
235 water content was determined by oven drying to constant weight at  $102^\circ\text{C}$  following the  
236 standard AOAC method, 950.46 (1997). The salt content was analyzed after sample  
237 homogenization (1g for fresh samples and 0.5g for salted samples) in 100mL of  
238 distilled water using an ULTRATURRAX (T25, IKA Labortechnik, Germany) at 9500rpm  
239 for 5min. Supernatant was filtered through membrane filters ( $45\mu\text{m}$ ) and a 500 $\mu\text{l}$  aliquot  
240 sample was taken and titrated in Chloride Analyzer equipment (Chloride Meter 926L,  
241 Ciba Corning, U.K.) (Carcel et al., 2007). All the analyses were performed in triplicate.  
242 As the ham's integrity cannot be altered before salting, the initial average values of salt  
243 and water content were obtained from 6 hams of the same breed purchased from the  
244 same supplier. The final salt gain ( $\Delta X_s$ ) and water loss ( $\Delta X_w$ ) were also calculated for  
245 each salting time.

## 246 **3. RESULTS AND DISCUSSION**

### 247 **3.1 ULTRASONIC ONLINE MONITORING OF THE HAM DRY SALTING PROCESS**

248 As an example of the ultrasonic signals obtained, Figure 2 shows the first and last  
249 signals of one transducer (T1) in the 11 days of the ham salting trial. On the one hand,  
250 the portion of signal received in zone A (dead zone) represents the transducer's own  
251 vibration after emission and also reflections of the ultrasonic wave on interfaces close  
252 to the transducer surface (for example, from the subcutaneous fat/lean meat interface).  
253 On the other hand, zone B includes the reflection of the wave on the meat/salt  
254 interface, and thus shows the arrival of the wavefront when it has crossed the whole  
255 sample twice. As can be observed in Figure 2, the TOF was shortened from the first to  
256 the last day of salting (11 days). This same behaviour, a decrease in the TOF as the  
257 salting time progressed, was observed in every experiment carried out (4, 10, 14, 16  
258 and 30 days). In the example of Figure 2, the ultrasonic signal at 11 days was  
259 displaced  $20.9\mu\text{s}$  (calculated by the ETM) to the left compared to the signal on day 0,  
260 which illustrates the shortening of the TOF and, consequently, the increase in velocity.  
261 This behaviour can be explained by the fact that an increase in ultrasonic velocity will  
262 occur as a result of either any increase in the material's elastic stiffness or any  
263 decrease in the density or both. Since density increases during salting (salt gain and  
264 water loss), the increase in velocity could be attributed to the meat's greater elastic  
265 stiffness due to the sample contracting and hardening during salting as a consequence  
266 of the salt gain and water loss. In this regard, De Prados et al. (2015, 2016) observed  
267 an ultrasonic velocity increase in brined and dry-salted *Biceps femoris* and  
268 *Longissimus dorsi* muscles, respectively. It has to be mentioned that the TOF reduction  
269 was not only ascribed to the increase of the ultrasonic velocity, but also to the ham's  
270 thickness reduction, due to the shrinkage caused by the coupled salting-dehydration.  
271 Thus, the shortening of the TOF observed during salting could be used to monitor the  
272 progress of the salting process and to determine the salt content modification. For that  
273 purpose, an accurate calculation of the TOF is required.

## 274 3.2 TIME OF FLIGHT CALCULATION BY USING THE ENERGY THRESHOLD 275 METHOD

276 Figure 3 depicts the TOF evolution of the ultrasonic signals corresponding to the two  
277 measurement points (T1 and T2) in the hams dry-salted for 10 and 16 days at 2°C.  
278 Similar behaviour was observed for the two measurement points in the remaining  
279 salting times tested (data not shown). Figure 3 shows a downward trend of the TOF  
280 during the salting time, which, as previously mentioned, is related to the increase in the  
281 meat's solid content and, consequently, to an increase in elastic stiffness. In addition,  
282 the initial TOF ( $TOF_0$ ) and the TOF evolution were different for both T1 and T2, which  
283 could be explained by considering the highly heterogeneous nature of the piece of ham  
284 from both compositional and structural points of view. Moreover, the different  $TOF_0$   
285 value could also be due to the differences in the ham's thickness.

286 Taking into account the ultrasonic signal displacement shown in Figure 2 and the  
287 compositional changes that take place during salting, a progressive decrease in the  
288 TOF during salting could be expected, coupled to the salt gain shown in Table 1.  
289 However, every salting experiment demonstrated several abrupt changes in the TOF  
290 evolution (Figure 3). These abrupt changes might not be related to compositional  
291 variations, as they occurred randomly and appeared upward and downward (Figure 3).  
292 In order to find the origin of this fact, the ultrasonic signals taken during salting were  
293 analysed. As an example, the ultrasonic signals (non-noise) (zone B, Figure 2) in T2,  
294 after 0, 127, 254 and 380h of the ham dry salted for 16 days were plotted in Figure 4.

295 As observed in Figure 4, the amplitude of the ultrasonic signals fluctuated during  
296 salting. The salt gain, water loss, sample contraction and the chemical and structural  
297 changes in the protein matrix during salting might be the reason for the amplitude  
298 fluctuation in the ultrasonic signal shown in Figure 4. In addition, the transducer-ham  
299 contact also may affect the amplitude of the ultrasonic signal. The fluctuations in the

300 signal amplitude mean that the energy threshold method detects the wavefront's arrival  
301 at a particular position and, when the signal amplitude decreases or increases over  
302 time, the new peak crossing the threshold can be randomly displaced backwards or  
303 forwards regardless of the salt gained. signal Different energy thresholds (0.05-1.2V)  
304 were evaluated in order to study their influence on the TOF assessment. However, the  
305 abrupt changes in the TOF evolution appeared in every case.

306 When an ultrasonic signal presents a high SNR, despite the amplitude fluctuations, the  
307 peak corresponding to the arrival wavefront will always exceed the established energy  
308 threshold [13], and thus, the ETM will always locate the arrival wavefront from the  
309 same peak, avoiding fluctuations in the TOF calculation. However, the ultrasonic waves  
310 found in this study were attenuated after crossing the ham twice, decreasing the SNR,  
311 and therefore, the fluctuations in the signal amplitude led to miscalculations of the TOF,  
312 resulting in the observed fluctuations in the  $\Delta$ TOF calculated by the ETM (Figure 3).  
313 Therefore, the ETM, which was successfully used by De Prados et al. (2016) for the  
314 purposes of monitoring the salting process in LD and BF muscles, was not suitable for  
315 application in the low SNR ultrasonic signals obtained during salting of whole hams.

### 316 **3.3 $\Delta$ TOF CALCULATION BY USING THE CROSS-CORRELATION METHOD**

317 An alternative to the ETM for analyzing the ultrasonic signals and calculating the TOF  
318 is that of the cross-correlation method (CCM). Leemans et al. (2009) used this method  
319 to calculate the TOF and detect foreign bodies in cheese. Similarly, Pallav et al. (2009)  
320 analyzed ultrasonic signals using the cross-correlation method to determine the TOF  
321 and detect foreign bodies and additives in food. This method compares two ultrasonic  
322 signals and calculates the time of flight variation ( $\Delta$ TOF) between them.

#### 323 **3.3.1 $\Delta$ TOF CALCULATION USING THE CROSS-CORRELATION METHOD** 324 **BETWEEN THE INITIAL ULTRASONIC SIGNAL AND THE REMAINING SIGNALS**

325 In the present section, the  $\Delta\text{TOF}_{2s}$  was calculated between the initial or reference  
326 ultrasonic signal (0h-RS) and the remaining signals measured during the dry-salting of  
327 hams (CCM-RS). Figure 5 shows the  $\Delta\text{TOF}$  decrease in hams salted for 14 and 30  
328 days at 2°C. Although the cross-correlation method was not conditioned by the  
329 amplitude fluctuations of the wavefront's arrival, abrupt changes in the  $\Delta\text{TOF}$  evolution  
330 were also found. The abrupt changes observed in Figure 5 could be explained by the  
331 change in the shape of the ultrasonic signal (signal distortion) during salting compared  
332 to the reference signal. As an example, Figure 6 shows both the RS and those  
333 obtained at 0, 200, 400 and 725h in the ham dry salted for 30 days at 2°C (T2). In  
334 Figure 6, only the zone of the ultrasonic signal corresponding to the reflection of the  
335 wave in the sample/salt interface is represented (non-noise, zone B, Figure 2). As can  
336 be appreciated, the pulse presents a clear distortion that can be ascribed to wave  
337 dispersion (variation of propagation properties with frequency), scattering and multipath  
338 propagation. As previously mentioned, this pulse distortion could be linked to the  
339 compositional changes (salt gain and water loss), the reduction in thickness and the  
340 protein denaturation suffered by the ham during salting.

341 As an example, the abrupt change observed in Figure 5 for the 14 days' salting trial  
342 was analyzed. Figure 7A shows the overlap of RS and the signal before the abrupt  
343 change (SBA) obtained by the cross-correlation method (where the maximum of the  
344 cross-correlation array is found), while Figure 7B shows the overlap of RS and the  
345 signal after the abrupt change (SAA). The maximum value obtained in the cross-  
346 correlation between RS-SBA (91.23 $\mu\text{s}$ ) was quite different to the one obtained in the  
347 cross-correlation between RS-SAA (94.04 $\mu\text{s}$ ), which gives rise to the abrupt change  
348 observed in Figure 5.

349 According to the results obtained in this section, the compositional and structural  
350 changes that take place in the meat during salting involve a distortion of the ultrasonic  
351 signal and, thereafter, a miscalculation of the  $\Delta\text{TOF}$  when CCM-RS is applied.

352 **3.3.2  $\Delta$ TOF CALCULATION USING THE CROSS-CORRELATION METHOD**  
353 **BETWEEN CONSECUTIVE SIGNALS**

354 From the analysis of the ultrasonic signals, it was observed that the distortion in the  
355 ultrasonic signal did not happen abruptly between consecutive signals (5min) but  
356 progressively during salting. Thus, in order to solve the problems found in the  
357 calculation of the  $\Delta$ TOF using the CCM-RS discussed in the previous section, the  
358 cross-correlation method was applied between consecutive (each one 5 min apart)  
359 ultrasonic signals (CCM-CS;  $n=0$ , no interpolation). Therefore, the  $\Delta$ TOF<sub>2s</sub> between  
360 each pair of signals was calculated and the relationship between the  $\Delta$ TOF and the  
361 salting time was represented by using the sum of the estimated  $\Delta$ TOF<sub>2s</sub>.

362 Figure 8 shows the  $\Delta$ TOF evolution, calculated using the CCM-CS  $n=0$ , in hams dry  
363 salted for 11 and 16 days. As can be observed, the  $\Delta$ TOF decreased during salting and  
364 no abrupt change was found. However, in the  $\Delta$ TOF of T1 during the 16 days' salting,  
365 an anomalous decrease trend was observed (Figure 8), which leads to a very different  
366  $\Delta$ TOF compared to T2. Initially, a normal decrease was found; however, at around 100  
367 h the rate of decrease fell abruptly. This anomalous behaviour was also observed in T1  
368 during the 30 days' salting (data not shown). Overall, the TOF estimation error is  
369 random, positive or negative; thus, it does not accumulate. However, for signals with  
370 very small differences between each other (only 5 min apart), i.e. TOF differences in  
371 the order of the discretization time in the digitized waveform, a bias in the CCM-CS  
372 algorithm that calculates the maximum in the correlation could appear, and lead to an  
373 accumulated error.

374 Thus, in order to minimize the possible error accumulation and to improve the  
375 resolution of the CCM for signals that are only very slightly displaced between each  
376 other, the sampling frequency could be increased, applying an interpolation method to  
377 the acquired signals. A different number of interpolation points ( $n$  from 1 to 5) were

378 considered in order to study their influence on the  $\Delta$ TOF calculation (data not shown),  
379  $n=3$  turning out to be the most appropriate one. Using the CCM-CS  $n=3$ , a progressive  
380 decrease in  $\Delta$ TOF was observed for every salting time studied (4, 10, 11, 14, 16 and  
381 30 days). Moreover, the differences between the final average  $\Delta$ TOF at measurement  
382 points T1 and T2 in the 16 and 30 days' salting experiments were drastically reduced  
383 when using the CCM-CS  $n=3$  ( $\Delta$ TOF<sub>avgT1-T2</sub> =  $-11.2 \pm 1.3 \mu\text{s}$  for 16 days and  $-17.3 \pm 0.1 \mu\text{s}$   
384 for 30 days) compared to the CCM-CS  $n=0$  ( $\Delta$ TOF<sub>avgT1-T2</sub> =  $-9.3 \pm 2.2 \mu\text{s}$  for 16 days and -  
385  $13.2 \pm 1.1 \mu\text{s}$  for 30 days) (Table 1). Non-significant ( $p > 0.05$ ) differences were observed  
386 between the final average  $\Delta$ TOF values using the CCM-CS  $n=3$  and the CCM-CS  $n=0$   
387 for the remaining salting times (4, 10, 11 and 14 days) (Table 1). Therefore, the CCM-  
388 CS  $n=3$  might reduce the accumulated error and allow the  $\Delta$ TOF calculation throughout  
389 the whole salting period. As the CCM-CS  $n=3$  involves an increase in the signal  
390 processing time, complementary methodologies will be explored in this paper.

### 391 **3.3.3 $\Delta$ TOF CALCULATION USING THE CROSS-CORRELATION METHOD** 392 **BETWEEN NON-CONSECUTIVE ULTRASONIC SIGNALS**

393 In order to reduce the computing requirements and the analysis time, the cross  
394 correlation method between non-consecutive ultrasonic signals (each one 1 h apart)  
395 (CCM-NCS) was evaluated. The objective is to increase the difference between the  
396 TOF of the two signals while keeping distortion as small as possible. Figure 9 shows  
397 the evolution of the  $\Delta$ TOF, calculated using the CCM-NCS, in hams dry salted for 11  
398 and 16 days (where the anomalous changes in the evolution of the  $\Delta$ TOF appeared  
399 when using the CCM-CS  $n=0$ ). The evolution of the  $\Delta$ TOF calculated using CCM-NCS  
400 behaved similarly to the  $\Delta$ TOF calculated using CCM-CS  $n=3$  for every salting time  
401 studied (4, 10, 11, 14, 16 and 30 days). Consequently, when using the CCM-NCS, the  
402 final average  $\Delta$ TOF were not significantly ( $p > 0.05$ ) different from those obtained using  
403 the CCM-CS  $n=3$  (Table 1), except for the ham salted for 16 days. Therefore, the

404 CCM-NCS could be an alternative method with which to calculate the  $\Delta$ TOF and to  
405 monitor the salting process of hams, reducing the signal analysis processing time and  
406 avoiding the miscalculations found when the ETM and the CCM-CS  $n=0$  were used.  
407 The accuracy of this method reflects the fact that time interval wave acquisition could  
408 be extended from 5 min to 1 hour without affecting the  $\Delta$ TOF assessment.

#### 409 **3.4 $\Delta$ TOF CALCULATION USING THE PHASE SPECTRUM METHOD**

410 Another alternative methodology used in the present study as a means of calculating  
411 the  $\Delta$ TOF was the phase spectrum method (PSM). When calculating the  $\Delta$ TOF by  
412 using the PSM, a similar trend was observed (Figure 10) in the T1 and T2  $\Delta$ TOF  
413 evolution for the entire salting experiment. Overall, non-significant ( $p>0.05$ ) differences  
414 were observed in the final average  $\Delta$ TOF values obtained using the PSM, the CCM-  
415 NCS and the CMM-CS  $n=3$  (Table 1). Therefore, any of these signal analysis methods  
416 could be used to calculate  $\Delta$ TOF and monitor the ham salting process.

#### 417 **3.5 PREDICTION OF THE SALT GAIN THROUGH THE $\Delta$ TOF**

418 As mentioned in section 3.1, the shortening of the TOF found during ham salting was  
419 influenced by the compositional changes (salt gain and water loss) as well as by the  
420 sample contraction and structural changes that take place during salting. When the  
421 final  $\Delta$ TOF value was related with the salt gain ( $\Delta X_s$ ) (Table 1), a great variability was  
422 found (data no-shown). In order to take into account the initial sample thickness, which  
423 can affect the relationship between the change in the time of flight and the salt gain, the  
424  $TOF_0$  was considered for the estimation of the salt gain. Therefore, the relationship  
425 between the salt gain and the  $\Delta$ TOF $\cdot$ TOF $_0$  was studied (Table 2). Since in previous  
426 sections, the CMM-CS  $n=3$ , CCM-NCS and PSM have been shown to be the most  
427 convenient ones with which to monitor the salting process, they were the methods  
428 chosen to calculate the  $\Delta$ TOF in every experiment. Using any of these methods to  
429 calculate the  $\Delta$ TOF, a significant ( $p<0.05$ ) relationship between the  $\Delta X_s$  and the



430  $\Delta\text{TOF} \cdot \text{TOF}_0$  was found, showing a high correlation coefficient ( $R^2=0.83$  for the CMM-  
431 CS  $n=3$ ,  $R^2= 0.93$  for the CCM-NCS and  $R^2=0.90$  for the PSM, Table 2). Consequently,  
432 the use of ultrasonic pulse-echo measurements, together with any of the three methods  
433 evaluated in this work (CMM-CS  $n=3$ , CCM-NCS and PSM), could be considered a  
434 reliable and effective technique for calculating the  $\Delta\text{TOF}$  and predicting the salt gain  
435 during ham dry-salting.

436 Several studies have shown the relationship between the ultrasonic velocity and the  
437 solid content in foodstuffs. In this regard, Valente et al. (2016) showed that the  
438 ultrasonic velocity increased along with a rise in the solid content during mango  
439 ripening. De Prados et al. (2015; 2016) reported that the ultrasonic velocity rose in pork  
440 meat (*Biceps femoris* and *Longissimus dorsi*) during salting. The ultrasonic velocity  
441 measurements require the sample's thickness be measured by means of some  
442 electronic gage, which could be considered a limitation in an industrial environment  
443 where hams are placed in a pile during dry-salting. By contrast, the pulse-echo TOF  
444 measurement presents a twofold advantage: the sample thickness does not need  
445 measuring and the ultrasonic transducers are only in contact with one of the ham  
446 surfaces, making the ultrasonic industrial application easier.

447

#### 448 **4. CONCLUSIONS**

449 The time of flight was progressively shortened during the ham dry-salting process. The  
450 energy threshold and the cross-correlation method between the initial signal and the  
451 remaining signals measured during the dry salting of ham were not able to provide  
452 reliable results for computing the the variation of the time of flight ( $\Delta\text{TOF}$ ). The lack of  
453 accuracy was linked to the the change in the signal amplitude, the limited SNR and the  
454 signal pulse distortion. The cross-correlation method between consecutive signals  
455 (5min apart) with interpolation  $n=3$ , between non-consecutive signals (1h apart) and

456 the phase spectrum method provided reliable results, being the most appropriate  
457 methods with which to calculate the  $\Delta$ TOF and monitor the ham salting process. By  
458 using any of these methods, the  $\Delta$ TOF weighted by the initial  $TOF_0$  was significantly  
459 ( $p < 0.05$ ) correlated to the salt gain in the hams.

460 Nowadays, quality control in pork ham industry lacks of nondestructive techniques to  
461 monitor the dry-salting process, which presents a high variability and complexity due to  
462 intrinsic (size, shape, fat content, pH ...) and extrinsic properties (air temperature and  
463 relative humidity, sample location in the pile layer ...) to the ham. Moreover, the high  
464 value of the ham pieces hinders the use of conventional destructive techniques to  
465 measure the salt content, due to their impact on the process cost. Thereby, the process  
466 control of ham dry-salting is largely conditioned by the background and empirical  
467 knowledge of industry technicians. Therefore, the industrial application of the ultrasonic  
468 experimental technique used in this work, based on laying the ham pieces over  
469 ultrasonic transducers and taking pulse-echo measurements, would contribute to a  
470 better process and product control. This strategy could be considered as feasible,  
471 robust and simple and emerges as a non-destructive and relatively affordable tool to  
472 monitor the dry-salting process of hams. The methodologies developed in this work  
473 would contribute to an accurate assessment of the variation of time of flight from the  
474 ultrasonic signal acquired during salting, which is critical for the estimation of the  
475 evolution of the salt gain. Future industrial implementation should address the analysis  
476 of the number of samples to be monitored, as well as the development of durable and  
477 low-cost electronics for signal generation, acquisition and processing.

478

## 479 **ACKNOWLEDGEMENTS**

480 This work was supported by the Spanish Ministerio de Economía y Competitividad  
481 (MINECO), Instituto Nacional de Investigación y Tecnología Agraria y Alimentaria  
482 (INIA) and European Regional Development Fund (ERDF 2014e2020) (project  
483 RTA2013-00030-C03-02), and by the Universitat Politècnica de València (UPV)  
484 through the FPI grant awarded to Marta de Prados (SP-1.2011-S1-2757).

485

486

487

488

489

490

## 491 **REFERENCES**

492 AOAC (1997). Association of Official Analytical Chemist. Official Methods of Analysis,  
493 16th Ed. Washington, DC.

494 Aparicio, C., Otero, L., Guignon, B., Molina-García, A.D., Sanz, P.D. (2008). Ice  
495 content and temperature determination from ultrasonic measurements in partially  
496 frozen foods. *Journal of Food Engineering* 88, 272-279.

497 Awad, T., Sato, K. (2002). Acceleration of crystallisation of palm kernel oil in oil-in-  
498 water emulsion by hydrophobic emulsifier additives. *Colloid Surface B.* 25, 45-53.

499 Benedito, J., Mulet, A., Velasco, J., Dobarganes, M.C. (2002). Ultrasonic assessment  
500 of oil quality during frying. *Journal of Agriculture and Food Chemistry* 50, 4531-4536.

501 Cárcel, J. A., Benedito, J., Bon, J., Mulet, A. (2007). High intensity ultrasound effects  
502 on meat salting. *Meat Science* 76, 611-619.

503 De Prados, M., García-Pérez, J.V., Benedito, J. (2015). Non-destructive salt content  
504 prediction in brined pork meat using ultrasound technology. *Journal of Food*  
505 *Engineering* 154, 39-48.

506 De Prados, M., García-Pérez, J.V., Benedito, J. (2016). Ultrasonic characterization and  
507 online monitoring of pork meat dry salting process. *Food Control* 60, 646-655.

508 Dixit, Y., Casado-Gavalda, M.P., Cama-Moncunill, R., Cama-Moncunill, X., Markiewicz-  
509 Kesztycka, M., Cullen, P.J., Sullivan, C. (2017). Developments and challenges in  
510 online NIR spectroscopy for meat processing. *Comprehensive Reviews in Food*  
511 *Science and Food Safety*, 16, 1172-1187.

512 Gomez Alvarez-Arenas, T.E. (2009a). Simultaneous determination of the ultrasound  
513 velocity and the thickness of solid plates from the analysis of thickness resonances  
514 using air-coupled ultrasound. *Ultrasonics 2009 Congress* 50, 104-109.

515 Gomez Alvarez-Arenas, T.E., Benedito, J., Corona, E. (2009b). Non-contact ultrasonic  
516 assessment of the properties of vacuum-packaged dry-cured ham. *2009 IEEE*  
517 *Ultrasonics Symposium*, 2541-2544.

518 Koc, A.B., Ozer, B. (2008). Nondestructive monitoring of renneted whole milk during  
519 cheese manufacturing. *Food Research International* 41, 745-750.

520 Koksel, F., Strybulevych, A., Page, J.H., Scanlon, M.G. (2014). Ultrasonic  
521 characterization of unyeasted bread dough of different sodium chloride concentrations.  
522 *Cereal Chemistry*, 91, 327-332.

523 Koksel, F., Strybulevych, A., Page, J.H., Scanlon, M.G. (2017). Ultrasonic investigation  
524 of the effects of composition on the volume fraction of bubbles and changes in their

525 relative sizes in non-yeasted gluten-starch blend doughs. *Journal of Food Engineering*,  
526 204, 1-7.

527 Leemans, V., Destain, M.F. (2009). Ultrasonic internal defect detection in cheese.  
528 *Journal of Food Engineering* 90, 333-340.

529 Nowak, K.W., Markowski, M. (2013). A comparison of methods for the determination of  
530 sound velocity in biological materials: A case study. *Ultrasonics*, 53, 923–927

531 Nowak, K.W., Markowski, M., Daszkiewicz, T. (2015). Ultrasonic determination of  
532 mechanical properties of meat products. *Journal of Food Engineering*, 147, 49-55.

533 Nowak, K.W., Markowski, M., Daszkiewicz, T. (2016). A modified ultrasonic method for  
534 determining the chemical composition of meat products. *Journal of Food Engineering*,  
535 180, 10-15.

536 Pallav, P., Hutchins, D.A., Gan, T.H. (2009). Air-coupled ultrasonic evaluation of food  
537 materials. *Ultrasonics* 49, 244-253.

538 Pérez-Santaescolástica, C., Fraeye, I., Barba, F.J., Gómez, B., Tomasevic, I., Romero,  
539 A., Moreno, A., Toldrá, F., Lorenzo, J.M. (2019). Application of non-invasive  
540 technologies in dry-cured ham: An overview. *Trends in Food Science and*  
541 *Technology*, 86, 360-374.

542 Piałucha, T., Guyott, C.C.H., Cawley, P. (1989). Amplitude spectrum method for the  
543 measurement of phase velocity. *Ultrasonics* 27, 270-279.

544 Povey M.J.W, Mason T.J. (1998). *Ultrasound in food processing*. Springer

545 Resa, P., Elvira, L., de Espinosa, F.M., Gonzalez, R., Barcenilla, J. (2009). On-line  
546 ultrasonic velocity monitoring of alcoholic fermentation kinetics. *Bioprocess and*  
547 *Biosystems Engineering* 32, 321-331.

548 Ronald L.; Mills, D. (2004). Signal analysis: time, frequency, scale, and structure. John  
549 Wiley & Sons.

550 Sachse, W., Pao. Y.H. (1978). On the determination of phase and group velocities of  
551 dispersive waves in solids. Journal of Applied Physics 49, 4320-4327.

552 Sarabia, E.G., Llata, J.R., Robla, S., Torre-Ferrero, C., Oria, J.P. (2013). Accurate  
553 estimation of airborne ultrasonic time-of-flight for overlapping echoes. Sensors 13,  
554 15465-15488.

555 Svilainis, L. (2016). Review of ultrasonic signal acquisition and processing techniques  
556 for mechatronics and material engineering. Solid State Phenomena, 251, 68-74.

557 Ting, C.H., Kuo, F.J., Lien, C.C., Sheng, C.T. (2009). Use of ultrasound for  
558 characterising the gelation process in heat induced CaSO<sub>4</sub>•2H<sub>2</sub>O tofu curd. Journal  
559 of Food Engineering 93, 101-107.

560 Toldrà, T. (2010). Handbook of Meat Processing. Blackwell Publishing. (2010). Iowa.

561 Valente, M., Prades, A., Laux, D. (2013). Potential use of physical measurements  
562 including ultrasound for a better mango fruit quality characterization. Journal of Food  
563 Engineering 116, 57-64.

564 Yucel, U., Coupland, J.N. (2010). Ultrasonic characterization of lactose dissolution.  
565 Journal of Food Engineering 98, 28-33.

566

567 **FIGURE CAPTIONS**

568 Figure 1. Experimental set-up for online ultrasonic pulse-echo measurements in hams  
569 during dry-salting.

570 Figure 2. Received signal (B-Scan) in pulse-echo mode for a ham sample at two  
571 different stages of salting (0 and 11 days). A: Dead zone. B: Echo coming from ham  
572 back surface.

573 Figure 3. Time of flight (TOF) evolution in the hams dry salted for 10 days (left) and 16  
574 days (right) at 2°C. TOF calculated using the Energy Threshold Method (ETM). T1  
575 and T2 refer to the two measurement points/transducers.

576 Figure 4. Change in the amplitude of the ultrasonic signals of T2 in the ham dry-salted  
577 for 16 days at 2°C (0, 127, 254 and 380h).

578 Figure 5. Time of flight variation ( $\Delta$ TOF) in the ham dry salted for 14 days (left) and 30  
579 days (right) at 2°C.  $\Delta$ TOF calculated using the CCM-RS. T1 and T2 refer to the two  
580 measurement points/transducers used. The arrow shows an abrupt change in the  
581  $\Delta$ TOF evolution. SBA and SAA refer to the signal before and after the abrupt  
582 change, respectively.

583 Figure 6. Signal of T2 in the ham dry-salted for 30 days at 2°C at different salting times  
584 (0, 200, 400 and 725h). Figure 7. Overlapping between the initial signal (RS) and  
585 that before (SBA; A) and after (SAA; B) the abrupt change shown in Figure 5,  
586 considering the maximum value of the cross-correlation array (transducer T1 in the  
587 ham dry salted for 14 days at 2°C).

588 Figure 7. Overlapping between the initial signal (RS) and that before (SBA; A) and after  
589 (SAA; B) the abrupt change shown in Figure 5, considering the maximum value of  
590 the cross-correlation array (transducer T1 in the ham dry salted for 14 days at 2°C).

591 Figure 8. Evolution of time of flight variation ( $\Delta$ TOF) in hams dry-salted for 11 days  
592 (left) and 16 days (right) at 2°C.  $\Delta$ TOF calculated using the CCM-CS n=0. T1 and T2  
593 refer to the two measurement points/ transducers used.

594 Figure 9. Evolution of time of flight variation ( $\Delta$ TOF) in the ham dry-salted for 11 days  
595 (left) and 16 days (right) at 2°C.  $\Delta$ TOF calculated using the CCM-NCS. T1 and T2  
596 refer to the two measurement points/transducers.

597 Figure 10. Evolution of time of flight variation ( $\Delta$ TOF) in hams dry-salted for 4 days  
598 (left) and 11 days (right) at 2°C.  $\Delta$ TOF calculated using the PSM. T1 and T2 refer to  
599 the two measurement points/transducers used.



**Table 1.** Final average time of flight variation ( $\Delta\text{TOF}$ ) calculated using the different signal analysis methods (CCM-CS n=0, CCM-CS n=3, CCM-NCS and PSM) and average salt gain ( $\Delta X_s$ )

Days	CCM-CS n=0( $\mu\text{s}$ )	CCM-CS n=3( $\mu\text{s}$ )	CCM-NCS( $\mu\text{s}$ )	PSM( $\mu\text{s}$ )	$\Delta X_s$ (%w.b.)
4	$-6.1 \pm 0.8^{a1}$	$-6.0 \pm 1.0^{j1}$	$-5.2 \pm 0.2^{e1}$	$-4.9 \pm 0.2^{m1}$	$0.71 \pm 0.04$
10	$-6.7 \pm 1.8^{ab2}$	$-7.3 \pm 1.2^{j2}$	$-7.6 \pm 1.5^{f2}$	$-7.0 \pm 0.9^{n2}$	$1.40 \pm 0.03$
11	$-10.6 \pm 1.7^{cd3}$	$-10.7 \pm 1.3^{k3}$	$-10.9 \pm 1.1^{g3}$	$-9.4 \pm 0.4^{o3}$	$2.55 \pm 0.21$
14	$-9.9 \pm 0.3^{bcd4}$	$-10.3 \pm 0.3^{k4}$	$-10.4 \pm 0.3^{g4}$	$-8.1 \pm 0.3^{n05}$	$2.11 \pm 0.38$
16	$-9.3 \pm 2.2^{abc6}$	$-11.2 \pm 1.3^{k6}$	$-14.1 \pm 0.1^{h7}$	$-13.2 \pm 0.2^{p67}$	$3.79 \pm 0.13$
30	$-13.2 \pm 1.1^{d9}$	$-17.3 \pm 0.1^{i10}$	$-17.3 \pm 0.2^{i10}$	$-16.1 \pm 0.2^{q10}$	$3.19 \pm 0.34$

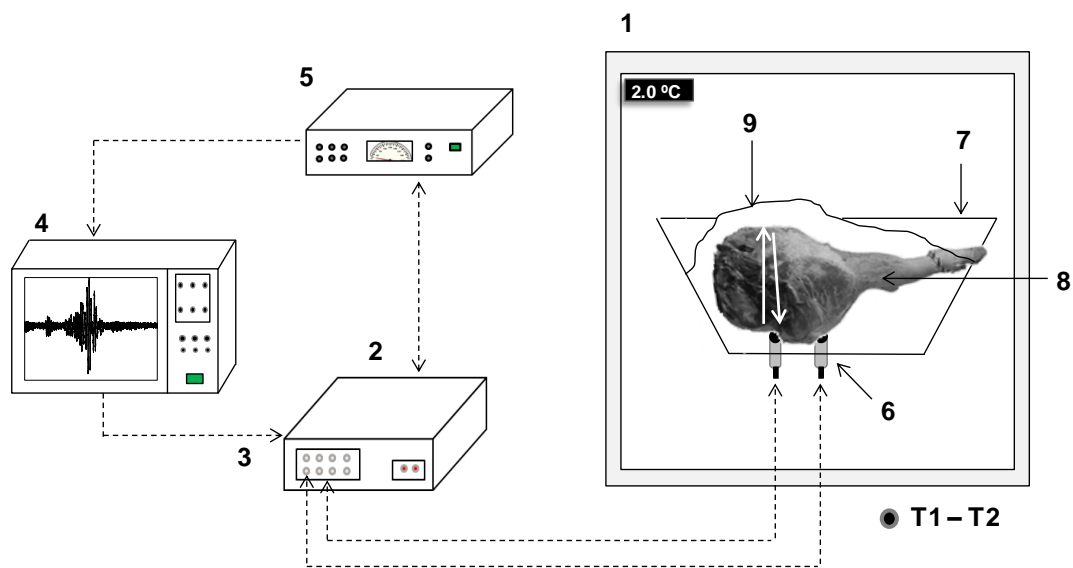
Mean values and standard deviations between T1 and T2. Different letters in the same column indicate significant ( $p < 0.05$ ) differences between salting times and different numbers in the same row significant ( $p < 0.05$ ) differences between the methods.

CCM-CS n=0 makes reference to the cross-correlation method between consecutive signals (every 5min) without interpolation, CCM-CS n=3 between consecutive signals (every 5min) with interpolation n=3 and CCM-NCS between non-consecutive signals (every 1h). PMS is the spectrum phase method between signals 5min apart.

**Table 2.** Linear regression models between the salt gain ( $\Delta X_s$ ) and the ultrasonic parameter ( $\Delta\text{TOF} \cdot \text{TOF}_0$ ) calculated using the different signal analysis methods (CCM-CS n=3, CCM-NCS and PSM).

Analysis method	Equation	$R^2$
CCM-CS n=3	$\Delta X_s = -0.0032 \Delta\text{TOF} \cdot \text{TOF}_0 - 0.039$	0.84
CCM-NCS	$\Delta X_s = -0.0028 \Delta\text{TOF} \cdot \text{TOF}_0 - 0.129$	0.93
PSM	$\Delta X_s = -0.0029 \Delta\text{TOF} \cdot \text{TOF}_0 - 0.032$	0.90

CCM-CS n=3 makes reference to the cross-correlation method between consecutive signals (each 5min) with interpolation n=3 and CCM-NCS between non-consecutive signals (each 1h). PMS is the spectrum phase method between signals separated 5min.



1. Cold Chamber 2. Multiplexer 3. USB 4. Data Acquisition Card-PC 5. Pulser-Receiver  
6. Transducers 7. Container 8. Ham 9. Salt

FIGURE 1

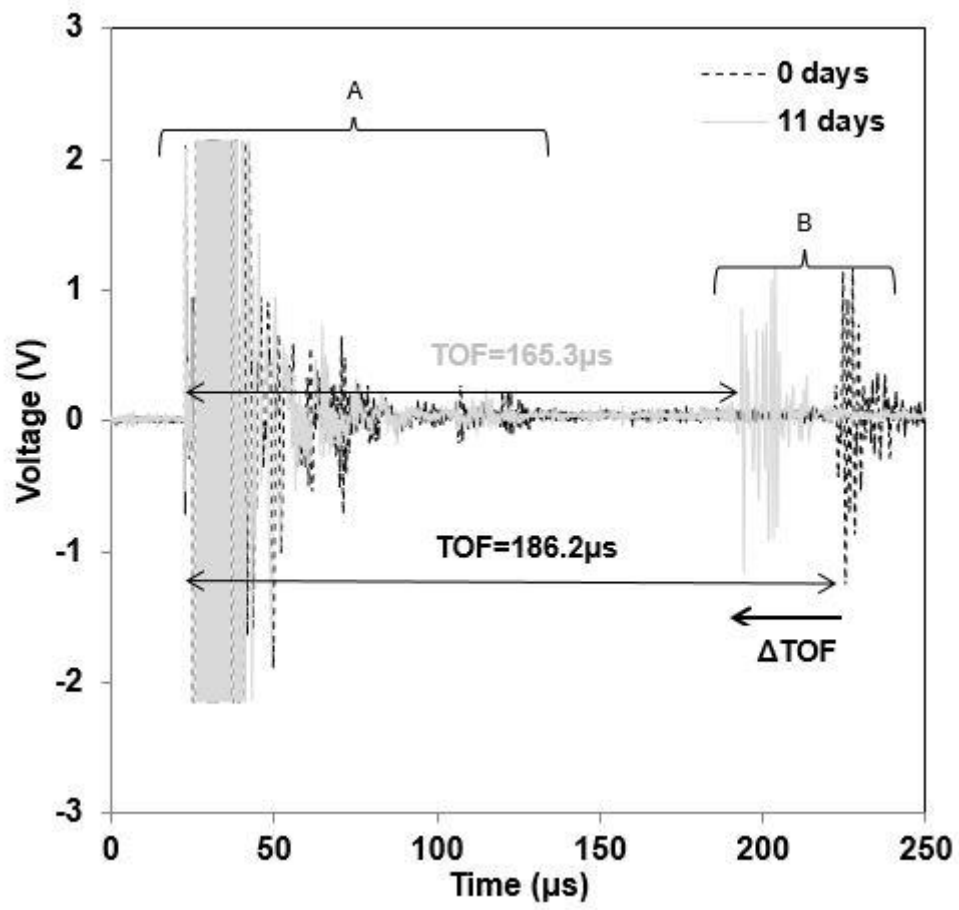


FIGURE 2

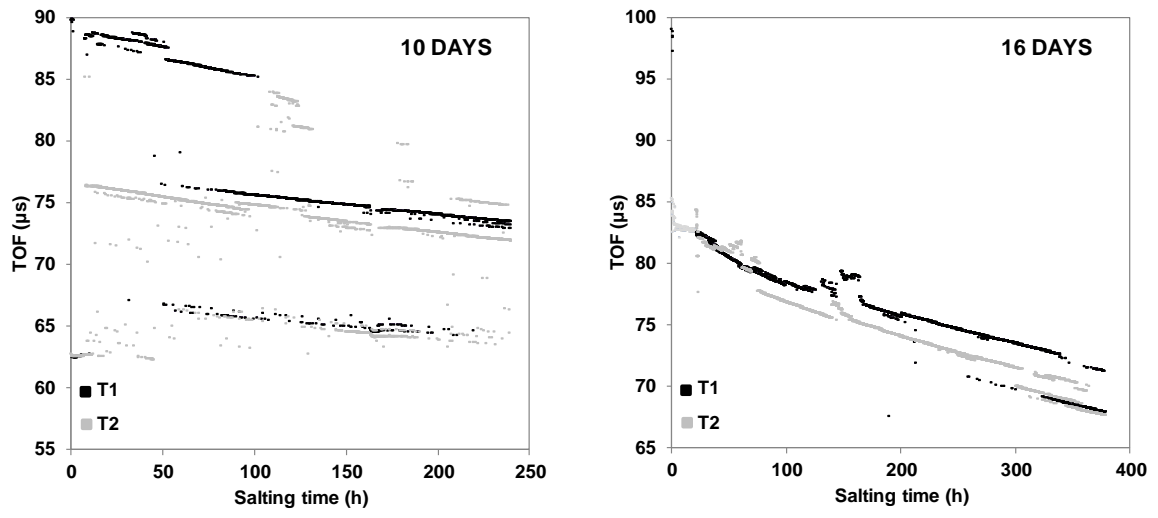


FIGURE 3

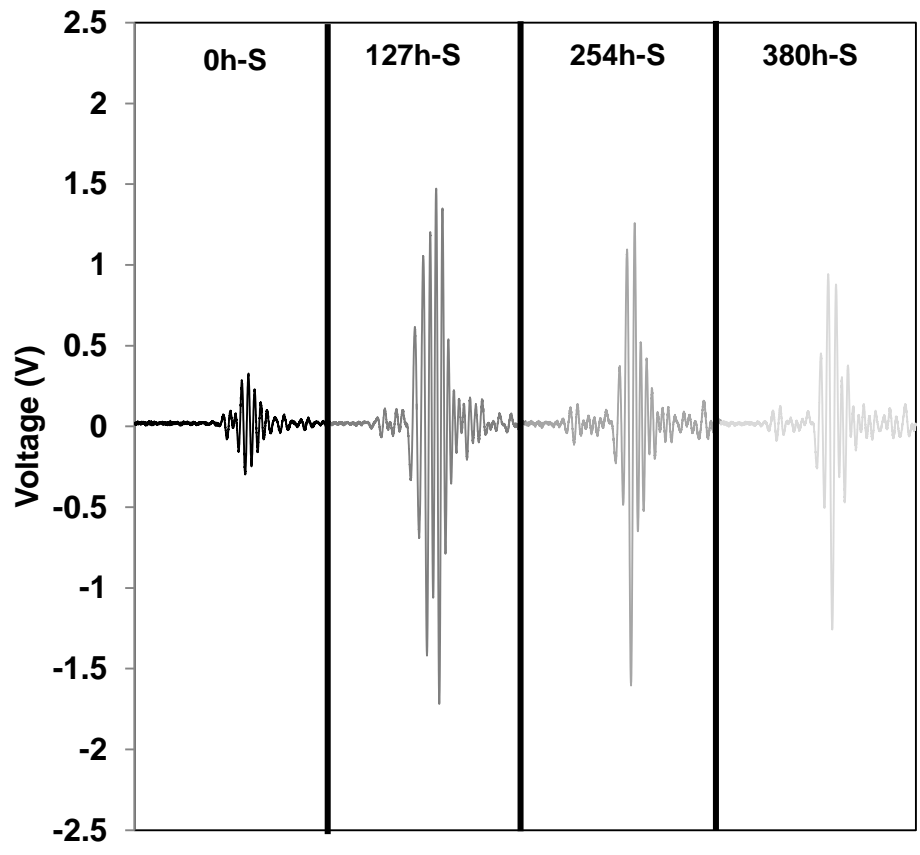


FIGURE 4

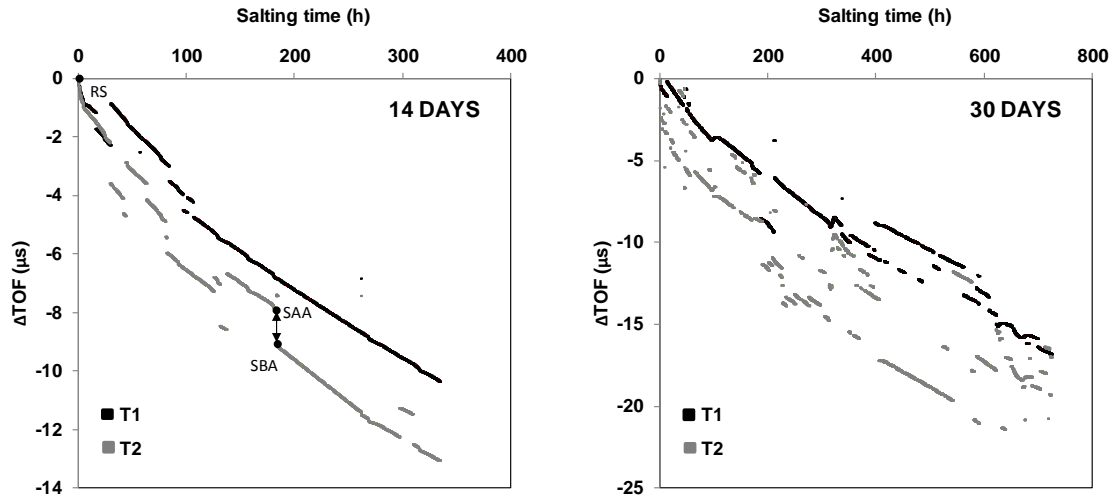
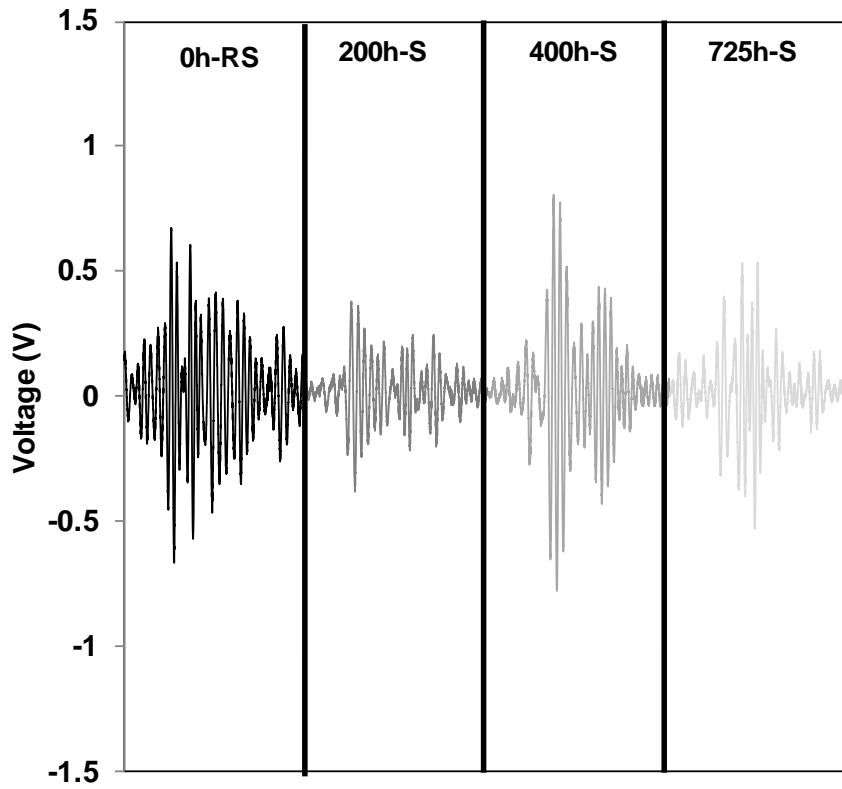


FIGURE 5



**FIGURE 6**

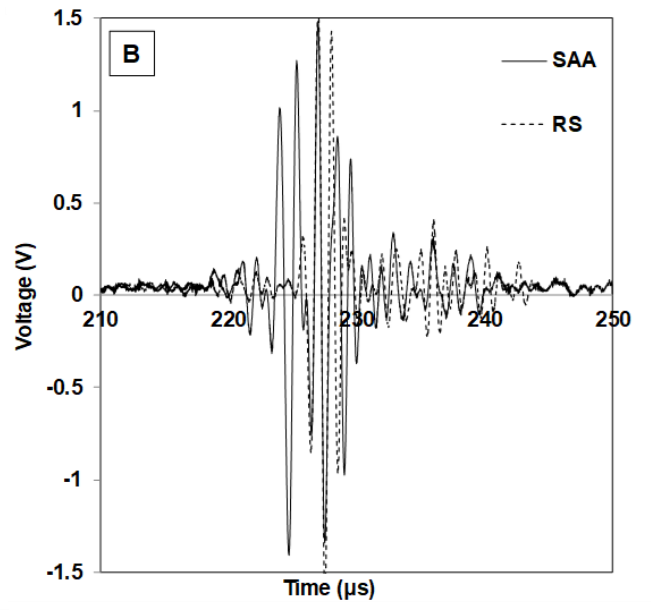
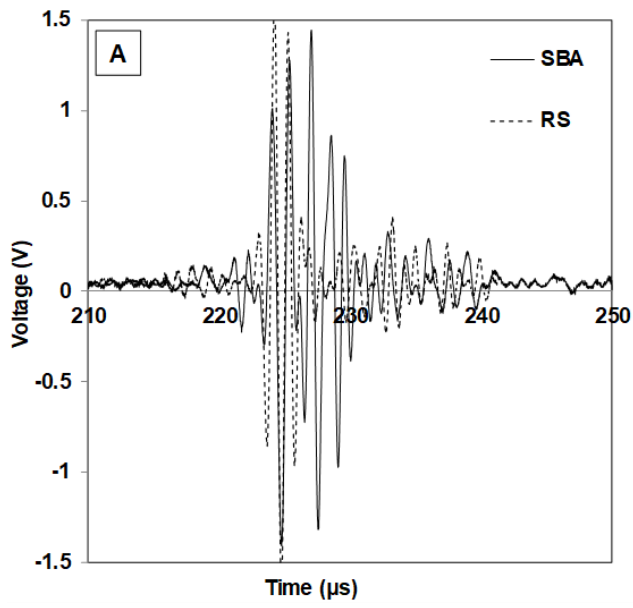


FIGURE 7



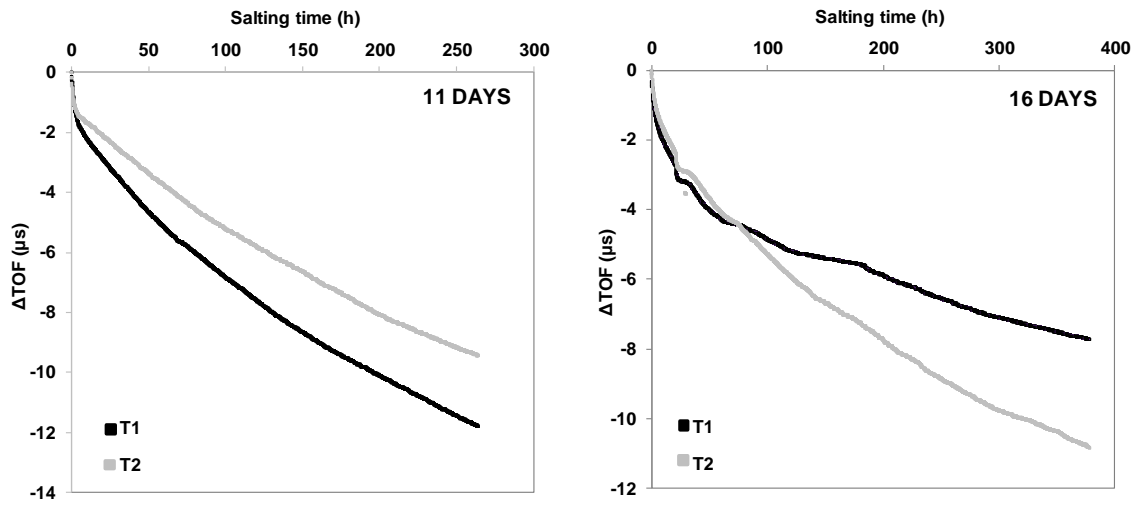


FIGURE 8

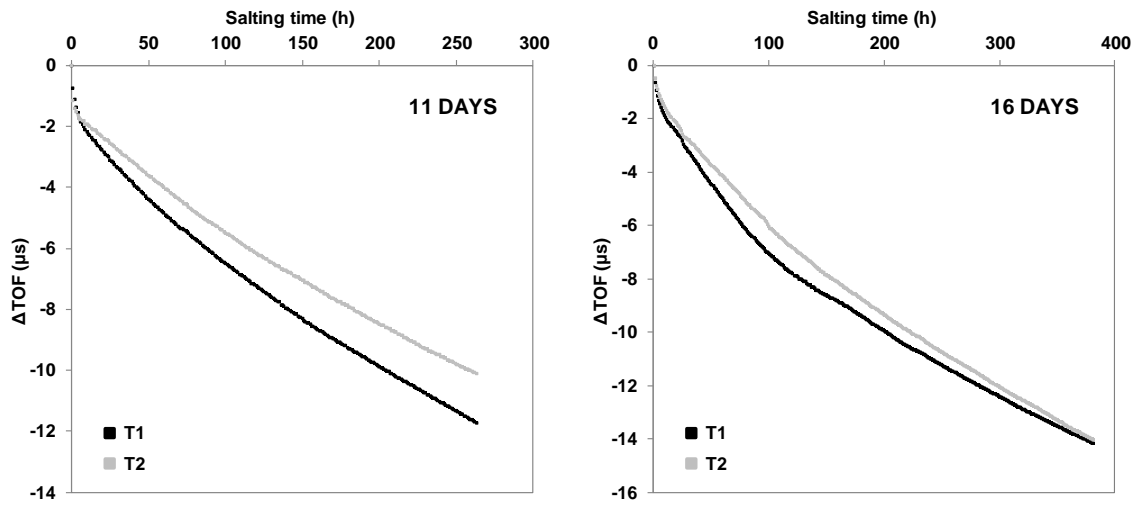


FIGURE 9

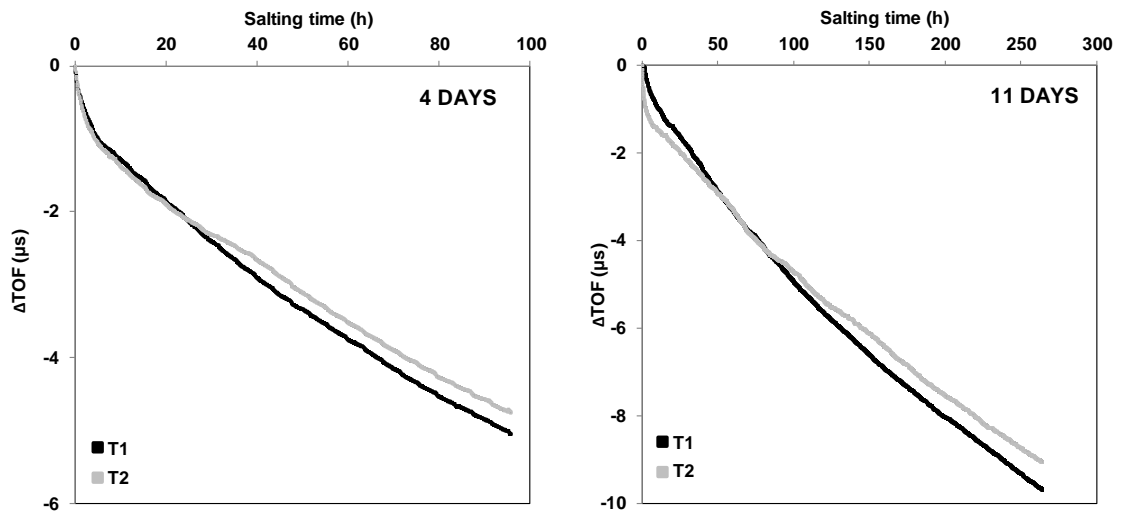


FIGURE 10